Chinese Journal of Catalysis 36 (2015) 1711–1718

available at www.sciencedirect.com

ScienceDirect

journal homepage: www.elsevier.com/locate/chnjc

Article

Preparation of mesoporous Fe-Cu mixed metal oxide nanopowder as active and stable catalyst for low-temperature CO oxidation

Ehsan Amini, Mehran Rezaei *

Institute of Nanoscience and Nanotechnology, Catalyst and Advanced Materials Research Laboratory, Chemical Engineering Department, Faculty of Engineering, University of Kashan, Kashan, Iran

ARTICLE INFO

Article history:
Received 13 April 2015
Accepted 25 May 2015
Published 20 October 2015

Keywords:
Iron oxide
Copper oxide
Metal oxide catalyst
Mesoporous nanopowder
CO oxidation
Sol-gel method

ABSTRACT

A series of mesoporous Fe-Cu mixed metal oxide nanopowders with different Cu/Fe molar ratios and high specific surface areas were synthesized via a simple, inexpensive, surfactant-free sol-gel route using propylene oxide as the gelation agent. The catalytic behavior of the nanopowders in low-temperature CO oxidation was investigated using a microreactor-gas chromatography system. The prepared materials were characterized by X-ray diffraction, N_2 adsorption-desorption, thermogravimetric-differential thermal analysis, temperature-programmed reduction, Fourier transform infrared spectroscopy, and transmission electron microscopy. These mesoporous Fe-Cu mixed metal oxide catalysts had nanocrystalline structures, narrow pore size distributions, and high surface areas; they showed high catalytic activities and stabilities in low-temperature CO oxidation. The addition of CuO to iron oxide affected the structure and catalytic performance of the iron oxide. The catalyst containing 15 mol% CuO had the highest specific surface area and catalytic activity, and showed high catalytic stability in low-temperature CO oxidation.

1. Introduction

There is a growing need for low-temperature CO oxidation catalysts with high stabilities and activities because of their numerous applications, e.g., in air purification devices for respiratory protection, CO_2 lasers, pollution control devices for reducing environmental and industrial emissions, and CO gas sensors, and for removal of CO from enclosed atmospheres such as those in space craft and submarines [1]. Noble metals (e.g., Au, Pt, Ru, and Pd) promoted with or supported on reducible oxides such as Fe_2O_3, CeO_2, MnO_2, SnO_2, and TiO_2 are the best candidates for low-temperature CO oxidation, and they are able to remove CO completely at ambient temperature [1–7]. However, noble metals are prone to sulfur poisoning and are expensive, therefore attention is increasingly being focused on the preparation of cheap transition-metal oxide catalysts such as CuO, Co_3O_4, and MnO_2 [8–16].

The catalytic activities of transition-metal oxides are lower than those of noble metals. In recent years, the application of nanoscience and nanotechnology in catalysis and the development of catalyst synthetic methods have led to improvements in the activities, selectivities, and stabilities of catalysts. Control of the nanoparticle shape and size and the use of nanoparticles with high surface areas as catalysts enable transition-metal oxide catalysts to be used instead of noble-metal catalysts.

Generally, transition-metal oxide nanoparticles are synthesized via chemical methods, using a series of surfactants containing groups such as amine and phosphorous groups to control the particle shape and size. These surfactants may not be removed entirely by calcination; they can remain on the catalyst surface and cover some of the active sites on the catalyst, and this has a negative effect on the catalytic properties

* Corresponding author. Tel: +98-31-55912469; Fax: +98-31-55559930; E-mail: rezaei@kashanu.ac.ir
DOI: 10.1016/S1872-2067(15)60922-6 | http://www.sciencedirect.com/science/journal/18722067 | Chin. J. Catal., Vol. 36, No. 10, October 2015

[17,18]. Avoidance of the use of surfactants in nanoparticle preparation is therefore important. In recent years, much attention has been focused on the synthesis of nanoparticles with high surface areas, using surfactant-free methods.

Among transition-metal oxides, iron oxide is an attractive candidate because it is cheap and efficient, especially in the removal of CO in burning cigarettes. The potential toxicity of other catalysts is a challenge. Furthermore, they have dual functions, based on their redox behavior in the presence of oxygen, and lattice oxygen loss in the absence of oxygen.

However, pure Fe_2O_3 has poor catalytic activity for CO oxidation at low temperature. Structural modifications of the Fe_2O_3 lattice by doping with copper oxide improve the catalytic activity of Fe_2O_3 at low temperatures [8,9].

In our previous work [19], we reported the synthesis of Fe-Cu mixed metal oxide nanopowders via a sol-gel route using propylene oxide as a gelation agent and $FeCl_3{\cdot}6H_2O$ as the Fe precursor in aqueous solution. CO oxidation reactions over the synthesized nanopowders were investigated in detail. The results showed that moderate catalytic activity was achieved in low-temperature CO oxidation.

Epoxides are cyclic ethers, and they are much more reactive than simple ethers because of ring strain. Epoxides are used as acid scavengers in organic synthesis. They act as a proton scavenger through protonation of the epoxide oxygen, and then irreversible ring opening by nucleophilic attack of an anionic conjugate base. This process is shown in Eq. (1):

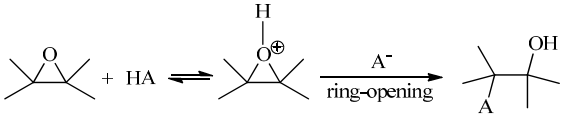

(1)

The aqua ion $[Fe(H_2O)_6]^{3+}$ is a strong acid, and epoxides can be easily protonated by strong acids. Propylene oxide therefore consumes protons from the hydrated Fe(III) species, as shown in Eq. (2):

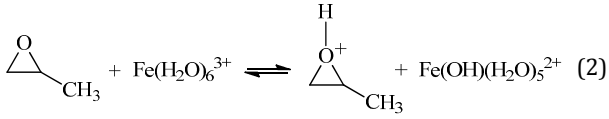

(2)

The Fe(III) complex on the right-hand side of Eq. (2) can undergo further hydrolysis and condensation to form more-condensed Fe(III) oxide species, as shown in Eq. (3):

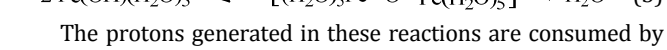

(3)

The protons generated in these reactions are consumed by protonation of the epoxide. The protonated epoxide can then be irreversibly ring opened via nucleophilic attack by Cl^- in solution. This process is shown in Eq. (4):

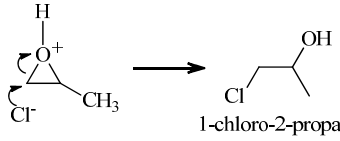

(4)

This process leads to elimination of protons from solution and causes further hydrolysis of the Fe(III) complex, leading to formation of a monolithic gel.

Cl^- ions adversely affect catalytic performances [20]. There was no washing step to remove Cl^- ions in our sol-gel method. Furthermore, Cl^- ions are not removed by catalyst calcination, therefore they remain on the catalyst surface and cover some active sites, leading to decreased catalytic activity.

Here, we report the preparation of mesoporous Fe-Cu mixed metal oxide nanopowders with different Cu/Fe molar ratios using $Fe(NO_3)_3{\cdot}9H_2O$ as the Fe precursor. However, based on the mechanism of gel formation when $Fe(NO_3)_3{\cdot}9H_2O$ is used as the Fe precursor, we cannot use water as the solvent. This is because, under the same conditions, water is a better nucleophile than the nitrate ion, therefore the protonated species in Eq. (2) could be preferentially ring opened by water. This leads to the proposed scenario shown in Eq. (5):

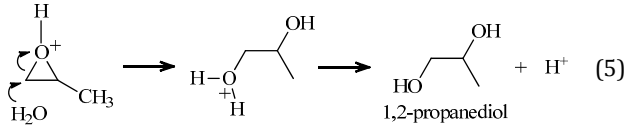

(5)

Here, the water attacks a ring carbon and is then deprotonated to give 1,2-propanediol and regenerate a proton. A proton is regenerated, therefore a gel is not formed.

In this work, we therefore used ethanol as the solvent and $Fe(NO_3)_3{\cdot}9H_2O$ as the Fe precursor for the preparation of mesoporous Fe-Cu mixed metal oxide nanopowders with different Cu/Fe molar ratios and high specific surface areas. The method is a simple, inexpensive, and surfactant-free sol-gel route. In addition, low-temperature CO oxidation over the prepared samples was investigated in detail. The effects of the Cu/Fe molar ratio, calcination temperature, and catalyst stability in the presence of water vapor and CO_2 were also studied.

2. Experimental

2.1. Materials

$Fe(NO_3)_3{\cdot}9H_2O$ and $Cu(NO_3)_2{\cdot}3H_2O$ were used as the Fe and Cu precursors, respectively. Propylene oxide and absolute ethanol were used as the gelation agent and solvent, respectively. All the starting materials were used without further purification.

2.2. Catalyst preparation

Fe-Cu mixed metal oxide nanopowders with different Cu/Fe molar ratios were synthesized via a simple sol-gel route using propylene oxide as a gelation agent. In a typical synthesis, $Fe(NO_3)_3{\cdot}9H_2O$ (10 mmol) and a calculated amount of $Cu(NO_3)_2{\cdot}3H_2O$ were dissolved in an appropriate amount of absolute ethanol at room temperature. After stirring for 15 min, a calculated amount of propylene oxide (propylene oxide/(Fe + Cu) molar ratio = 11) was added to the prepared solution. Gel formation occurred within 5 min. The resulting gel was aged at room temperature for 1 h, dried at 80 °C for 48 h, and calcined at various temperatures, with a ramp rate of 3 °C/min, for 5 h in air. The nominal CuO contents were 10, 15, and 20 mol%, and the corresponding catalysts were denoted by FeCu10, FeCu15, and FeCu20, respectively.

2.3. Catalyst characterization

X-ray diffraction (XRD) was performed using a PANalytical X'Pert-Pro X-ray diffractometer with a Cu K_α monochromatized radiation source and a Ni filter, in the scanning range 2θ = 20°–80°. Temperature-programmed reduction (H_2-TPR) was performed using an automatic instrument (Chemisorb 2750, Micromeritics) equipped with a thermal conductivity detector (TCD). In the TPR measurements, the catalyst (100 mg) was heated (10 °C/min) in a gas flow (30 mL/min) containing a mixture of H_2:Ar (10:90). Prior to the TPR experiments, the samples were heated in an inert atmosphere (Ar) at 200 °C for 1 h. The H_2 uptake during the reduction was measured using a TCD. Fourier-transform infrared (FTIR) spectroscopy (NEXus FTIR spectrophotometer) was performed using KBr pellets containing 1% by weight of the sample. The catalysts were examined using thermogravimetry (TG) and differential thermal analysis (DTA; Netzsch STA 409 system) at a heating rate of 10 °C/min in a static air atmosphere. Nitrogen adsorption/desorption analysis (BET method) was performed at −196 °C using an automated gas adsorption analyzer (Tristar 3020, Micromeritics). Transmission electron microscopy (TEM) was performed using a JEM-2100UHR instrument.

2.4. Catalytic activity tests

Catalytic activity tests for CO oxidation were performed in a continuous-flow fixed-bed quartz reactor at ambient pressure. The reactor was charged with 100 mg of the prepared catalyst sieved to 35–70 mesh. The reaction gases consisted of 20% O_2 and 2% CO, balanced with 78% inert gas. The catalysts were pretreated in 20% O_2 balanced with He at 300 °C for 2 h prior to the reaction. The activity tests were performed at different temperatures, in steps of 25 °C. The gas compositions of the reactants and products were analyzed on line using a gas chromatograph (Varian 3400) equipped with a TCD and a 5A molecular sieve column. The CO conversion (X_{CO}) was obtained using Eq. (6):

$$X_{CO} = (CO_{inlet} - CO_{outlet})/CO_{inlet} \times 100\% \quad (6)$$

3. Results and discussion

3.1. Catalyst characterization

Fig. 1 and 2 show the XRD patterns of the sol-gel-prepared Fe-Cu mixed metal oxide nanopowders with different Cu/Fe molar ratios calcined at various temperatures. The pattern of the pure Fe_2O_3 sample shows the reflections characteristic of rhombohedral hematite (α-Fe_2O_3) and cubic maghemite (γ-Fe_2O_3) iron oxide structures. The addition of 10 mol% CuO (FeCu10 sample) caused the diffraction peaks related to α-Fe_2O_3 to disappear, and peaks from $CuFe_2O_4$ appeared. These changes in the peak positions suggest the incorporation of Cu atoms into the α-Fe_2O_3 lattice and formation of spinel $CuFe_2O_4$. For FeCu15 and FeCu20, the corresponding diffraction patterns were similar to that of the FeCu10 sample. When the calcination temperature was increased to 400 °C, the sample diffraction patterns did not change. However, on further increasing the calcination temperature, the characteristic peak for α-Fe_2O_3 appeared. This indicates a phase transformation from γ-Fe_2O_3 to α-Fe_2O_3.

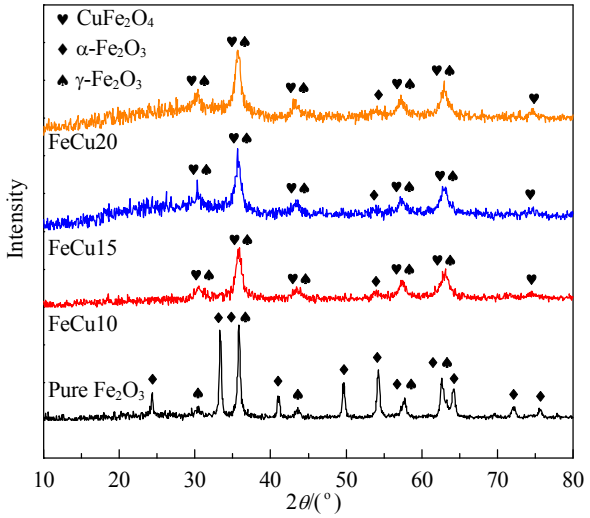

Fig. 1. XRD patterns of prepared Fe-Cu mixed metal oxide nanopowders with different Cu/Fe molar ratios, calcined at 300 °C.

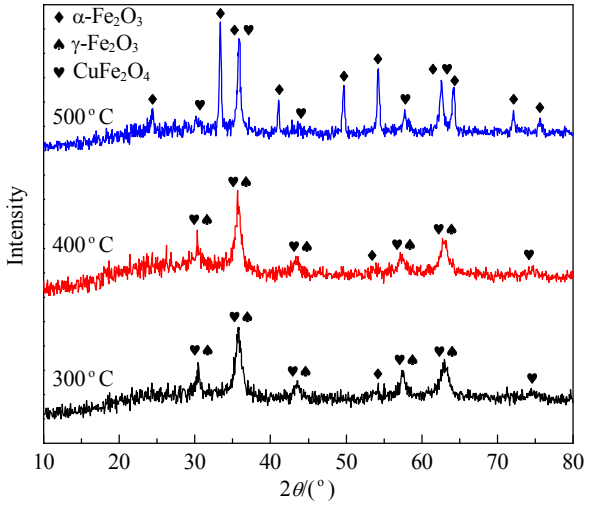

Fig. 2. XRD patterns of FeCu15 samples calcined at 300, 400, and 500 °C.

The average crystallite sizes were calculated from the half-widths of the main diffraction peaks, using the Scherrer formula; the results are shown in Table 1.

The H_2-TPR profiles of prepared catalysts with different CuO contents are shown in Fig. 3. The H_2-TPR profile of pure Fe_2O_3 shows two identified reduction peaks. The first peak, at 300–400 °C, corresponds to the reduction of Fe_2O_3 to Fe_3O_4, and the wide peak above 600 °C is related to the reduction of Fe_3O_4 to FeO and Fe(0) [21]. The reduction profile of the FeCu10 sample has a sharp peak at 200 °C. This peak is related to the reduction of CuO to Cu(0) [22]. The peaks corresponding to the reduction of Fe_2O_3 to Fe(0) in the FeCu10 sample were shifted to lower temperature compared with those of pure Fe_2O_3. This peak position shift shows that CuO promoted the reduction of Fe_2O_3 at low temperatures. Further increases in the CuO content (FeCu15 and FeCu20) increased the intensity

Table 1
Structural properties and catalytic activities of prepared catalysts.

Sample	Calcination temperature (°C)	Average crystalline size (nm)	Surface area (m^2/g)	Pore volume (cm^3/g)	Average pore size (nm)	T_{100} (°C)
Fe_2O_3	300	14	90.1	0.18	8.0	285
FeCu10	300	10	110.8	0.22	7.9	180
FeCu15	300	8	124.5	0.21	6.7	170
FeCu20	300	11	107.8	0.25	9.3	200
FeCu15	400	15	84.7	0.18	8.7	185
FeCu15	500	28	17.9	0.09	20.3	200

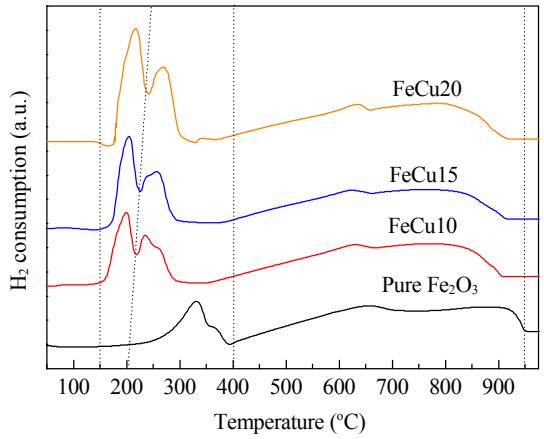

Fig. 3. H_2-TPR profiles of prepared catalysts with various CuO contents, calcined at 300 °C.

of the peak related to CuO reduction.

Fig. 4 shows the FTIR spectra of the as-prepared and calcined FeCu15 samples. The wide peak in the as-prepared sample at 3395 cm^{-1} is ascribed to the stretching vibration of the hydroxyl groups of adsorbed water and ethanol; the peak intensity decreased after calcination. The weak band in this region in the spectrum of the calcined sample is related to adsorbed water. The peak at 1628.7 cm^{-1} is attributed to adsorbed water; the peak intensity decreased after calcination. The peak at 1081.9 cm^{-1} is ascribed to the C–O stretching vibration; it vanished after calcination. The two peaks at ~2926.5 cm^{-1} are attributed to the stretching vibrations of CH_3 and CH_2 groups in propylene oxide (and compounds derived from it during the sol-gel process); these peaks disappeared after calcination. The peak at 1377.2 cm^{-1}, attributed to the bending vibration of CH_3, also disappeared after calcination. The two peaks in the region 400–600 cm^{-1} are related to metal–oxygen bond vibrations at octahedral and tetragonal holes in the spinel structure; these peaks were sharpened by calcination at 300 °C.

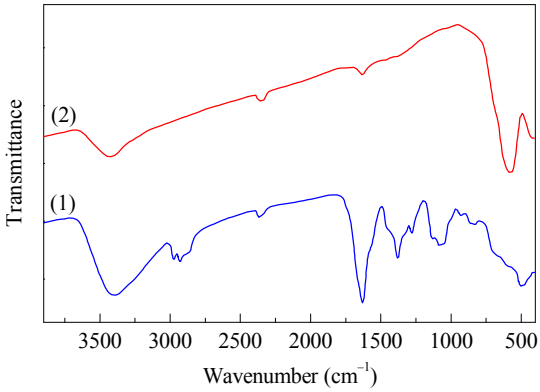

Fig. 4. FTIR spectra of as-prepared FeCu15 sample (1) and FeCu15 sample calcined at 300 °C (2).

Fig. 5 shows the TG-differential thermogravimetry (DTG) and DTA curves of the as-prepared FeCu15 sample. The DTA curve shows a broad endothermic peak in the region 50 to 150 °C, related to mass losses in several step in the TG curve. These mass losses are related to the evaporation of water adsorbed on the surface and water trapped in the pores. An exothermic peak appears in the DTA curve at 150–250 °C, corresponding to a rapid mass loss in the TG curve. This exothermic peak is attributed to propylene oxide and its combustion products. There is an exothermic peak in the region 250–350 °C, which is related to a weight loss in the TG curve in this region. This mass loss arises from removal of residual hydroxyl groups and crystallization of metal hydroxides to metal oxides. The weight loss from 350 to 450 °C in the TG curve, corresponding to the endothermic peak in the DTA curve in this region, is related to the decomposition of nitrate from the Fe and Cu precursors.

Fig. 6 shows the N_2 adsorption/desorption isotherms and pore size distributions of the prepared catalysts, with different CuO loadings and calcined at various temperatures. The structural characteristics of all the samples are listed in Table 1.

The isotherms of all the samples are type IV, based on the

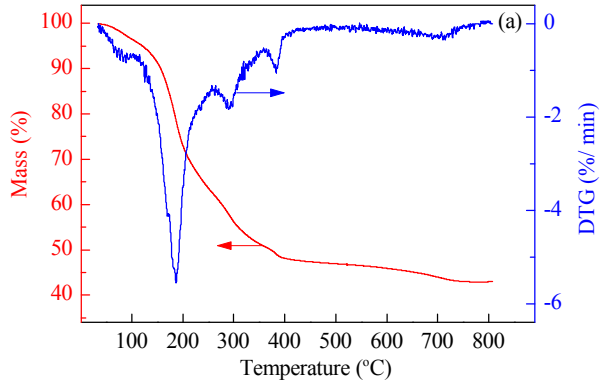

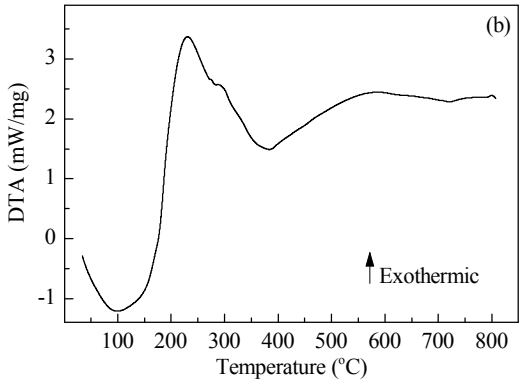

Fig. 5. TG-DTG (a) and DTA (b) curves of as-prepared FeCu15 catalyst.

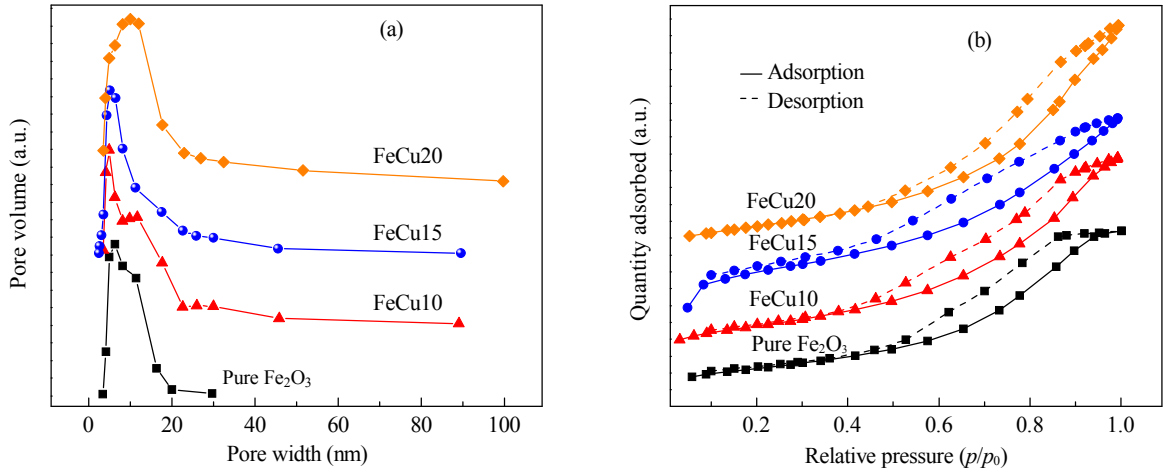

Fig. 6. Pore size distributions (a) and N_2 adsorption/desorption isotherms (b) of all prepared catalysts calcined at 300 °C.

International Union of Pure and Applied Chemistry classification scheme; this shows that they are mesoporous materials with complex structures made up of interconnected networks of different shapes and pore sizes. The hysteresis loops are type H2, which is characteristic of a solid containing particles crossed by nearly cylindrical channels, or consisting of agglomerated (unconsolidated) or aggregated (consolidated) spherical particles with nonuniform shapes or pore sizes. The pore size distribution curves show that samples with different CuO loadings calcined at 300 °C have mesoporous structures with narrow size distributions; this indicates good pore homogeneity. The pore size distributions of FeCu15 sample calcined at various temperatures are shown in Fig 7. The figure shows that with increasing calcination temperature, the pore sizes increase, accompanied by decreases in the surface areas. The pore walls collapse and form larger pores with increasing calcination temperature. The data in Table 1 show that the specific surface areas of all the samples calcined at 300 °C are higher than that of pure Fe_2O_3 (90.1 m^2/g). In addition, with increasing CuO content up to 15 mol%, the specific surface area increases to 124.5 m^2/g. However, on increasing of the CuO loading to 20 mol%, the specific surface area decreases. The results show that increasing the calcination temperature decreased the specific surface area of the FeCu15 sample, as a result of pore destruction and particle sintering.

TEM images at different magnifications and electron diffraction pattern of FeCu15 calcined at 300 °C are shown in Fig. 8. The electron diffraction pattern shows several distinct concentric rings, indicating a polycrystalline structure. The TEM im-

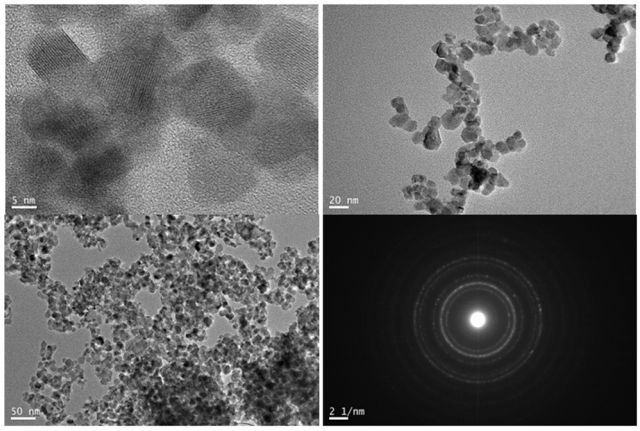

Fig. 8. TEM images at different magnifications and electron diffraction pattern of FeCu15 sample calcined at 300 °C.

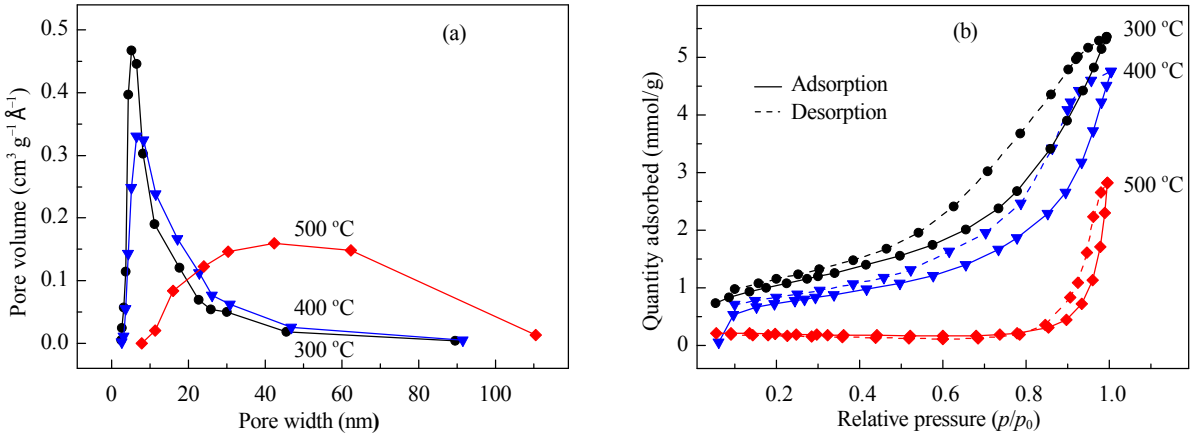

Fig. 7. Pore size distributions (a) and N_2 adsorption/desorption isotherms (b) of FeCu15 sample calcined at 300, 400, and 500 °C.

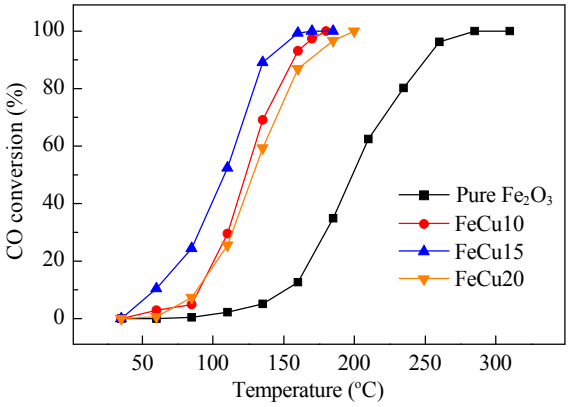

Fig. 9. Catalytic activities in CO oxidation over prepared catalysts with various Cu/Fe molar ratios, calcined at 300 °C.

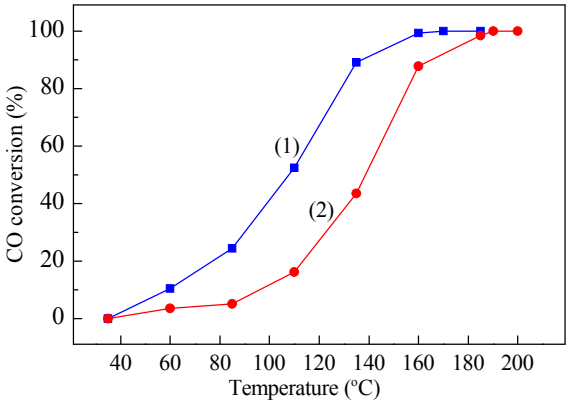

Fig. 11. Catalytic activities of FeCu15 sample prepared in this work (1) and in our previous work (2), both calcined at 300 °C.

ages clearly show a nanocrystalline structure with particle sizes in the range 5–15 nm.

3.2. Catalytic activity tests

Fig. 9 shows the CO conversions over prepared catalysts with various CuO contents, calcined at 300 °C. The results show that the addition of CuO to Fe_2O_3 significantly increases the catalytic activity at low temperatures. CuO and pure Fe_2O_3 form Fe-Cu mixed metal oxides with high surface areas and catalytic activities through a synergistic effect. The FeCu15 sample had the highest surface area and catalytic activity, with total CO conversion at 170 °C. However, the catalytic activity decreased with further increases in the CuO content. Excess CuO generally covers the catalyst surface and causes growth of CuO particles with low specific surface areas and catalytic activities.

Fig. 10 shows the CO oxidation curves for FeCu15 sample calcined at different temperatures. The catalytic activity decreased with increasing calcination temperatures. In general, with increasing calcination temperature, the pore walls are destroyed and larger pores are formed. The FeCu15 sample calcined at 300 °C, with a specific surface area of 124.5 m^2/g, showed the highest catalytic activity (T_{100} = 170 °C, Table 1), and the sample calcined at 500 °C with a specific surface area of 17.9 m^2/g showed the lowest catalytic activity (T_{100} = 200 °C).

Fig. 11 shows the catalytic activity results for the FeCu15 prepared in this work and those for FeCu15 prepared in our previous work [19]. The graphs show that the catalytic activity in low-temperature CO oxidation of the FeCu15 sample prepared in this work using $Fe(NO_3)\cdot 9H_2O$ as the Fe precursor is higher than that of the FeCu15 sample prepared in our previous work using $FeCl_3\cdot 6H_2O$ as the Fe precursor. NO_3^- ions are decomposed during calcination and removed from the catalyst surface. In contrast, Cl^- ions are not decomposed; they remain on the surface of the catalyst and act as a poison by covering some of the active sites, thereby decreasing catalytic activity.

The catalyst stability and effects of feed composition and reaction time on the catalytic activity of FeCu15 were investigated by performing the CO oxidation reaction for various time at 150 °C, using various feed compositions; the results are shown in Fig. 12. The results show that the prepared catalyst had good stability during reaction for 50 h, without any decrease in CO conversion. Addition of 10% CO_2 to the feed composition caused a small drop in catalytic activity initially, and then the activity remained unchanged for 50 h on stream. The addition of 10% H_2O vapor to the feed composition containing CO_2 further reduced the initial catalytic activity, which then remained unchanged for 50 h. The initial decrease in catalytic

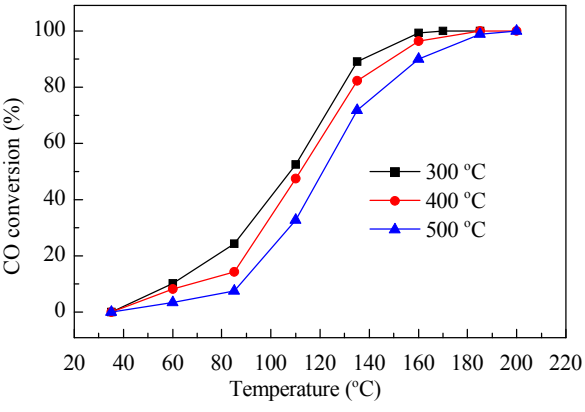

Fig. 10. Catalytic activities in CO oxidation over FeCu15 sample calcined at 300, 400, and 500 °C; gas hourly space velocity = 60 000 mL g^{-1} h^{-1}.

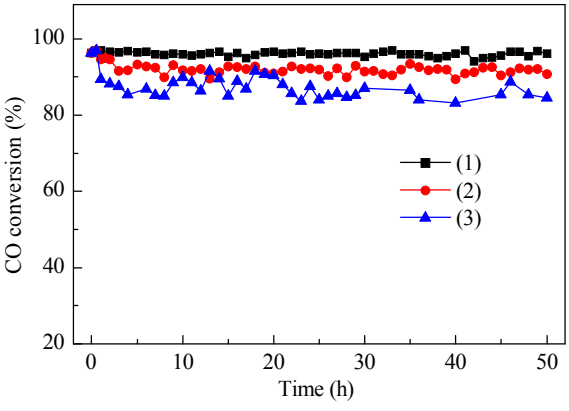

Fig. 12. Long-term stability of FeCu15 catalyst calcined at 300 °C in the presence of different feed compositions: net feed (1), feed with 10% CO_2 (2), and feed with 10% CO_2 and 10% H_2O (3).

activity can be attributed to the formation of carbonate species on the catalyst surface and the occupation of active sites on the catalyst by CO_2 and H_2O molecules. These results indicate that Fe-Cu mixed metal oxide catalysts prepared using a sol-gel method are stable in low-temperature CO oxidation, even in the presence of deactivating agents such as H_2O vapor and CO_2.

4. Conclusions

Mesoporous Fe-Cu mixed metal oxide nanopowders with different Cu/Fe molar ratios and high specific surface areas were synthesized via a simple, inexpensive, and surfactant-free sol-gel route, using propylene oxide as the gelation agent. The powders have mesopores with narrow pore size distributions, and nanocrystalline structures with particle sizes in the range 5–15 nm. The results show that the catalytic activity of pure Fe_2O_3 in low-temperature CO oxidation is low, but the addition of CuO to Fe_2O_3 significantly increases the catalytic activity at low temperatures. CuO and pure Fe_2O_3 form Fe-Cu mixed metal oxides with high surface areas and increased catalytic activities through a synergistic effect. The FeCu15 sample has the highest surface area and catalytic activity, with complete CO conversion at 170 °C. The results indicate that the prepared catalyst has good stability during reaction for 50 h, without any decrease in CO conversion. In addition, the Fe-Cu mixed metal oxide catalyst prepared via a sol-gel method is stable in low-temperature CO oxidation, even in the presence of deactivating agents such as H_2O vapor and CO_2.

Acknowledgments

The authors gratefully acknowledge the supports from University of Kashan by Grant No. 158426/13.

References

[1] Gardner S D, Hoflund G B, Schryer D R, Schryer J, Upchurch B T, Kielin E J. *Langmuir*, 1991, 7: 2135
[2] Haruta M, Tsubota S, Kobayashi T, Kageyama H, Genet M J, Delmon B. *J Catal*, 1993, 144: 175
[3] Wang S R, Huang J, Zhao Y Q, Wang S P, Wang X Y, Zhang T Y, Wu S H, Zhang S M, Huang W P. *J Mol Catal A*, 2006, 259: 245
[4] Schryer D R, Upchurch B T, Sidney B D, Brown K G, Hoflund G B, Herz R K. *J Catal*, 1991, 130: 314
[5] Schryer D R, Upchurch B T, Van Norman J D, Brown K G, Schryer J. *J Catal*, 1990, 122: 193
[6] Han Y F, Kahlich M J, Kinne M, Behm R J. *Appl Catal B*, 2004, 50: 209
[7] Zhu H Q, Qin Z F, Shan W J, Shen W J, Wang J G. *J Catal*, 2004, 225: 267
[8] Cao J L, Wang Y, Yu X L, Wang S R, Wu S H, Yuan Z Y. *Appl Catal B*, 2008, 79: 26
[9] Cheng T, Fang Z Y, Hu Q X, Han K D, Yang X Z, Zhang Y J. *Catal Commun*, 2007, 8: 1167
[10] Cao J L, Shao G S, Wang Y, Liu Y P, Yuan Z Y. *Catal Commun*, 2008, 9: 2555
[11] Biabani-Ravandi A, Rezaei M. *Chem Eng J*, 2012, 184: 141
[12] Guo Q, Liu Y. *Appl Catal B*, 2008, 82: 19
[13] Sadeghinia M, Rezaei M, Amini E. *Korean J Chem Eng*, 2013, 30: 2012
[14] Li J, Zhu P F, Zuo S F, Huang Q Q, Zhou R X. *Appl Catal A*, 2010, 381: 261
[15] Li G N, Li L, Shi J J, Yuan Y Y, Li Y S, Zhao W R, Shi J L. *J Mol Catal A*, 2014, 390: 97
[16] Li G N, Li L, Li Y S, Shi J L. *New J Chem*, 2015, 39: 1742
[17] Kuhn J N, Tsung C K, Huang W Y, Somorjai G A. *J Catal*, 2009, 265: 209
[18] Borodko Y, Jones L, Lee H, Frei H, Somorjai G. *Langmuir*, 2009, 25: 6665
[19] Amini E, Rezaei M, Sadeghinia M. *Chin J Catal*, 2013, 34: 1762

Graphical Abstract

Chin. J. Catal., 2015, 36: 1711–1718 doi: 10.1016/S1872-2067(15)60922-6

Preparation of mesoporous Fe-Cu mixed metal oxide nanopowder as active and stable catalyst for low-temperature CO oxidation

Ehsan Amini, Mehran Rezaei *
University of Kashan, Iran

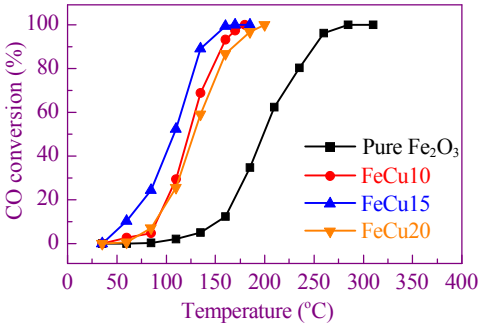

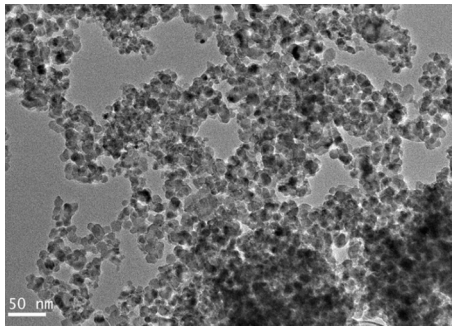

Mesoporous Fe-Cu mixed metal oxide nanopowders with different Cu/Fe molar ratios and high specific surface areas were synthesized via a sol-gel route. The nanopowders exhibited good catalytic behavior in low-temperature CO oxidation.

[20] Yentekakis I V, Lambert R M, Konsolakis M, Kallithrakas-Kontos N. *Catal Lett*, 2002, 81: 181
[21] Yang Q J, Choi H, Al-Abed S R, Sionysios D D. *Appl Catal B*, 2009, 88: 462
[22] Fierro G, Lojacono M, Inversi M, Porta P, Lavecchia R, Cioci F. *J Catal*, 1994, 48: 709